Antitumor alkyl-lysophospholipid analogue edelfosine induces apoptosis in pancreatic cancer by targeting endoplasmic reticulum

Consuelo Gajate[1,2], Marcia Matos-da-Silva[1,2], EL Habib Dakir[1], Rosalba I. Fonteriz[3], Javier Alvarez[3] and Faustino Mollinedo[1]

[1]Instituto de Biología Molecular y Celular del Cáncer, Centro de Investigación del Cáncer, CSIC-Universidad de Salamanca, Campus Miguel de Unamuno, E-37007 Salamanca, Spain; [2]Unidad de Investigación, Hospital Universitario de Salamanca, Campus Miguel de Unamuno, E-37007 Salamanca, Spain; and [3]Departamento de Bioquímica y Biología Molecular, Instituto de Biología y Genética Molecular, Universidad de Valladolid-CSIC, Ramón y Cajal 7, E-47005 Valladolid, Spain

Running title: Endoplasmic reticulum as pancreatic cancer target

Keywords: Endoplasmic reticulum stress; apoptotic signaling; pancreatic cancer; xenograft animal model; alkyl-lysophospholipid analogue; edelfosine.

Correspondence: Dr. Consuelo Gajate, Instituto de Biología Molecular y Celular del Cáncer, Centro de Investigación del Cáncer, CSIC-Universidad de Salamanca, Campus Miguel de Unamuno, E-37007 Salamanca, Spain. Phone: (+34) 923-294806; Fax: (+34) 923-294795; E-mail: cgajate@usal.es

Abstract

Pancreatic cancer remains as one of the most deadly cancers, and responds poorly to current therapies. The prognosis is extremely poor, with a 5-year survival of less than 5%. Therefore, search for new effective therapeutic drugs is of pivotal need and urgency to improve treatment of this incurable malignancy. Synthetic alkyl-lysophospholipid analogues (ALPs) constitute a heterogeneous group of unnatural lipids that promote apoptosis in a wide variety of tumor cells. In this study, we found that the anticancer drug edelfosine was the most potent ALP in killing human pancreatic cancer cells, targeting endoplasmic reticulum (ER). Edelfosine was taken up in significant amounts by pancreatic cancer cells, and induced caspase- and mitochondrial-mediated apoptosis. Pancreatic cancer cells show a prominent ER, and edelfosine accumulated in this subcellular structure, inducing a potent ER stress response, with caspase-4, BAP31 and c-Jun NH_2-terminal kinase (JNK) activation, CHOP/GADD153 upregulation, and phosphorylation of eukaryotic translation initiation factor 2 α-subunit (eIF2α), that eventually led to cell death. Oral administration of edelfosine in xenograft mouse models of pancreatic cancer induced a significant regression in tumor growth, and an increase in apoptotic index, as assessed by TUNEL assay and caspase-3 activation in the tumor sections. The ER stress-associated marker CHOP/GADD 153 was visualized in the pancreatic tumor isolated from edelfosine-treated mice, indicating a strong *in vivo* ER stress response. These results suggest that edelfosine exerts its proapoptotic action in pancreatic cancer cells, both *in vitro* and *in vivo*, through its accumulation in the ER, which leads to ER stress and apoptosis. Thus, we propose that endoplasmic reticulum could be a key target in pancreatic cancer, and edelfosine may constitute a prototype for the development of a new class of antitumor drugs targeting endoplasmic reticulum.

Introduction

Pancreatic adenocarcinoma is one of the most aggressive cancers. Pancreatic cancer is often detected at an advanced stage and prognosis is extremely poor, with a median survival of 4-6 months (Li *et al.*, 2004). It represents ~10% of all gastrointestinal malignancies (Neoptolemos *et al.*, 2003), and it is the fourth most common cause of death in Western countries (Jemal *et al.*, 2007). Most patients with diagnosed pancreatic cancer do not benefit from surgery and frequently need palliative chemotherapy (van Riel *et al.*, 1999). Standard treatments for advanced disease include 5-fluorouracil and gemcitabine. However, even gemcitabine, considered the gold standard for pancreas cancer, has a response rate of less than 20% (Li *et al.*, 2004).

The endoplasmic reticulum (ER) is an organelle responsible for several important cellular functions, including protein and lipid biosynthesis, post-translational modification, folding and assembly of newly-synthesized secretory proteins and cellular calcium store. Various conditions can disturb ER functions, leading to a series of events collectively termed ER stress. An excessive ER stress leads to an accumulation of misfolded proteins in the ER lumen, that initiates the unfolded protein response (UPR) to restore normal ER function. However, persistent ER stress can switch the cytoprotective functions of UPR into cell death promoting mechanisms, leading to the triggering of ER-dependent apoptotic cascades. One of the features of pancreatic cells is a highly developed ER, apparently due to a heavy engagement in insulin secretion (Oyadomari *et al.*, 2002). ER stress is directly related to pancreatic cell dysfunction and death by apoptosis, during the progression of type 1 and type 2 diabetes mellitus and Wolfram syndrome (Fonseca *et al.*, 2009). Nevertheless, ER stress sensors do not directly cause cell death, but rather initiate the activation of downstream molecules such as CHOP (C/EBP homologus protein)/growth arrest and DNA damage-inducible gene 153 (GADD153) or c-Jun NH_2-terminal kinase (JNK), which further push the cell down the path of death. Three main pathways of ER stress-induced apoptosis are known: 1) upregulation of the transcription factor CHOP/GADD153 (Ron and Habener, 1992); 2) JNK activation (Urano *et al.*, 2000); 3) activation of caspase-12 in murine systems or caspase-4 in human cells (Hitomi *et al.*, 2004). These three pathways all end in caspase cascade activation followed by the induction of apoptosis.

Accumulation of unfolded proteins, leading to ER stress, can be induced by anticancer chemotherapeutic agents such as bortezomib (Fribley *et al.*, 2004), geldanamycin (Mimnaugh *et al.*, 2004), cisplatin (Mandic *et al.*, 2003), and cannabinoids (Carracedo *et al.*, 2006). Also, chronic exposure to long-chain free fatty acids induces ER stress and cell death in pancreatic beta-cells (Cunha *et al.*, 2008). Synthetic alkyl-lysophospholipid analogues (ALPs) are a novel class of unnatural lipids with promising anticancer activity, including clinically relevant drugs such as miltefosine, perifosine and erucylphosphocholine, that act at the cell membrane level (Gajate and Mollinedo, 2002; Mollinedo *et al.*, 2004). Edelfosine (1-*O*-octadecyl-2-*O*-methoxy-*rac*-glycero-3-phosphocholine, ET-18-OCH_3), considered the ALP prototype compound, has been shown to induce apoptosis in malignant cells in a rather selective way, through the involvement of lipid rafts and ER (Gajate *et al.*, 2004; Gajate *et al.*, 2000b; Gajate *et al.*, 2009a; Gajate and Mollinedo, 2001; Gajate and Mollinedo, 2007; Mollinedo *et al.*, 1997; Mollinedo and Gajate, 2006; Mollinedo and Gajate, 2010; Nieto-Miguel *et al.*, 2007).

Because pancreatic cancer cells show prominent ER (Klimstra *et al.*, 1992; Skarda *et al.*, 1994), we wondered whether edelfosine might be active against pancreatic cancer by targeting ER. Hence, we investigated the *in vitro* and *in vivo* action of edelfosine on pancreatic cancer as well as its mechanism of action. In this work, using different *in vitro* and *in vivo* experimental approaches, we show that edelfosine behaves as an effective anticancer agent that induces apoptotic cell death of pancreatic cancer cells, via accumulation of the drug at the ER, leading to ER stress response and eventually to apoptosis.

Results

Induction of apoptosis by edelfosine and other ALPs in human pancreatic cancer cells

We have recently found that the pharmacologically relevant concentration in plasma of edelfosine ranges between 10-20 μM (Estella-Hermoso de Mendoza *et al.*, 2009; Mollinedo *et al.*, 2010). Thus, we first analyzed the proapoptotic activity of edelfosine and different ALPs, including perifosine, miltefosine, and erucylphosphocholine (ERPC), at 10 and 20 μM, on a number of human pancreatic cancer cells. Our data indicated that edelfosine induced cell death in a dose- and time-dependent manner (Figure 1a). We found that edelfosine was the only ALP that promoted apoptosis at 10 μM in all pancreatic cancer cells (Figure 1a), whereas the other ALPs did not induce cell killing at this drug concentration, even after 72 h incubation (data not shown). At 20 μM, we found that ALPs ranked edelfosine > perifosine >> ERPC ≥ miltefosine in their capacity to induce apoptosis in the pancreatic BxPC-3, Capan-2, CFPAC-1 and HuP-T4 cancer cells (Figure 1b). We included in our analysis the structurally related inactive edelfosine analogue 1-*O*-octadecyl-*rac*-glycero-3-phosphocholine (ET-18-OH) (Gajate *et al.*, 1998; Mollinedo *et al.*, 1997), in which the methoxy group in the *sn*-2 position was replaced by an OH group. We found that, save edelfosine and perifosine, the other ALP analogues rendered similar figures of apoptosis as ET-18-OH (Figure 1b). Thus, edelfosine and perifosine were the only ALPs with proapoptotic activity against pancreatic cancer cells.

Edelfosine accumulates in the ER of pancreatic cancer cells

Because edelfosine behaved as the most potent ALP in inducing cell death in pancreatic cancer cells, we next analyzed its mechanism of action. First, we found that that all pancreatic cancer cell lines assayed incorporated high amounts of drug (Figure 1c). Next, we found that the new fluorescent edelfosine analogue Et-BDP-ET (1-*O*-[11'-(6''-ethyl-1'',3'',5'',7''-tetramethyl-4'',4''-difluoro-4''-bora-3a'',4a''-diaza-*s*-indacen-2''-

yl)undecyl]-2-*O*-methyl-*rac*-glycero-3-phosphocholine) (Mollinedo *et al.*, 2011) accumulated in the ER of HuP-T4 and Capan-2 cells (Figure 2a), as assessed using a version of RFP targeted to ER lumen (erRFP; endoplasmic reticulum-targeted red fluorescence protein), which completely colocalized with the ER marker calreticulin (Klee and Pimentel-Muinos, 2005). Incorporation of fluorescent Et-BDP-ET into the cells was blocked by adding the parent drug edelfosine (data not shown), thus behaving as a reliable edelfosine fluorescent analogue to visualize the subcellular location of the drug "*in situ"*.

Edelfosine induces ER stress response in pancreatic cancer cells

We next analyzed whether this drug induced an ER stress response leading to apoptosis in HuP-T4 cells. To this aim, we examined the effect of edelfosine on a number of ER stress-associated markers, including caspase-4, CHOP/GADD153, BAP31, GRP78/BiP and eukaryotic translation initiation factor 2 α-subunit (eIF2α). Human caspase-4 is a potential homologue of murine caspase-12 involved in ER stress (Hitomi *et al.*, 2004). As shown in Figure 2b, edelfosine treatment induced caspase-4 activation, as assessed by cleavage of procaspase-4 into the 20-kDa active form. CHOP/GADD153 activates transcription of several genes that potentiate apoptosis during ER stress (Oyadomari and Mori, 2004). CHOP/GADD153 expression, together with phosphorylation of eIF2α, were strongly induced in HuP-T4 cells following edelfosine treatment (Figure 2b). BAP31 is an integral membrane protein of the ER that regulates ER-mediated apoptosis through its caspase-8-mediated cleavage into a 20-kDa fragment, which directs proapoptotic signals between ER and mitochondria (Breckenridge *et al.*, 2003). Here, we found that BAP31 was cleaved into the p20 fragment upon edelfosine treatment (Figure 2b). Edelfosine did not upregulate Grp78/BiP (Figure 2b), a major ER chaperone that binds Ca^{2+} and promotes tumor proliferation, survival, metastasis, and resistance to a wide variety of therapies (Li and Lee, 2006). ER stress has been shown to induce activation of Bax (Zong *et al.*, 2003), and we found Bax activation in response to edelfosine treatment in pancreatic cancer cells, by using an anti-Bax monoclonal antibody that recognized the active form of Bax (Figure 2b). Previous studies have shown that ASK1-mediated JNK activation is crucial for ER-induced apoptosis (Nishitoh *et al.*, 2002). We found here that edelfosine induced a potent and sustained activation of JNK in all pancreatic cancer cells lines (Figure 2c). Pre-incubation with the caspase-4 inhibitor z-LEVD-fmk, or the specific JNK inhibitor SP600125, diminished edelfosine-induced apoptosis (Figure 2, d and e), when used at concentrations that prevented edelfosine-induced caspase-4 and JNK activation (data not shown). These data reveal that edelfosine accumulates in the ER of pancreatic cancer cells, and induces an ER stress response.

Edelfosine induces sXBP1 expression

When the UPR is induced during ER stress, the ER-resident transmembrane kinase/RNase inositol-requiring enzyme 1 (IRE1) is activated, leading to site-specific splicing to form spliced *XBP1* mRNA (*sXBP1*) by removing a 26-nucleotide internal sequence from unspliced *XBP1* (*uXBP1*) mRNA. The presence in this 26-nucleotide fragment of a *Pst*I restriction site further allowed us to distinguish between both forms by restriction analysis of PCR-amplified cDNA, and thus to assay for ER stress response activation (Hirota *et al.*, 2006). By RT-PCR we found the induction of *sXBP1* mRNA following treatment of BxPC-3 cells with 20 µM edelfosine (Figure 3a). Similar data were obtained by *Pst*I restriction analysis (data not shown). Because sXBP1 is a key modulator of the UPR, our results suggest that edelfosine induces ER stress and UPR signaling in pancreatic cancer cells.

UPR is known as a prosurvival response to reduce the accumulation of unfolded proteins and restore normal ER function. However, when persistent, ER stress can switch the cytoprotective functions of UPR into cell death promoting mechanisms. Preincubation of BxPC-3 cells for 1 h with different concentrations (up to 2 mM) of dithiothreitol (DTT), a widely-used ER and UPR stress inducer, before edelfosine addition, did not cause apoptosis (Supplementary Figure S1a). Pretreatment of BxPC-3 cells with DTT for 1 h, followed by washing off DTT and subsequent incubation with edelfosine for 24 h slightly reduced the percentage of apoptotic cells as compared with cells treated only with edelfosine without DTT pretreatment (Supplementary Figure S1a). However, this reduction was not statistically significant ($P = 0.15$).

By using the primers indicated in Supplementary data, the *sXBP1* form generates a 414 bp fragment, while the *uXBP1* form generates a 440-bp fragment, which contains a *Pst*I restriction site leading to the generation of two bands of 294 and 146 bp following *Pst*I digestion. However, *sXBP1*, lacking the restriction site is resistant to *Pst*I digestion, and hence only one band of 414 bp is obtained. As shown in Supplementary Figure S1b, *sXBP1* was readily observed in pancreatic cancer cells incubated with DTT, edelfosine, or DTT+edelfosine. Edelfosine by itself was a potent inducer of *sXBP1* (Supplementary Figure S1b). These results suggest that edelfosine activates UPR by activating the IRE1-XBP1 branch of the UPR pathway. Taken together, our data might suggest that previous induction of UPR does not inhibit edelfosine-induced apoptosis. Thus, our data suggest that edelfosine action on ER is persistent and leads to the triggering of apoptotic signals that may overcome protective UPR mechanisms.

Edelfosine induces changes in ER calcium level

Because ER plays a critical role in controlling cellular Ca^{2+} levels, we next analyzed how edelfosine affected $[Ca^{2+}]_{ER}$. Reconstitution of ER-targeted aequorin with a semisynthetic prosthetic group, coelenterazine n, required previous depletion of Ca^{2+} of the ER to prevent aequorin consumption during reconstitution (Montero *et al.*, 1997b). Once aequorin was reconstituted, the ER was refilled again with Ca^{2+} by perfusing the cells with extracellular medium containing 1 mM Ca^{2+}. This led to an increase in $[Ca^{2+}]_{ER}$, that reached a steady-state of around 250 μM within 3-4 min in BxPc-3 cells

(Figure 3a). Addition of edelfosine induced a large increase in $[Ca^{2+}]_{ER}$, which nearly doubled the previous values within 10-15 min (Figure 3a). This effect was time dependent. Adding edelfosine 15 min before starting ER refilling induced a huge $[Ca^{2+}]_{ER}$ increase reaching levels above 900 µM (Figure 3b). However, longer incubation times (30 and 60 min) with edelfosine induced only a two-fold increase of the steady-state ER calcium levels (Figure 3b). These results suggest a progressive decrease in the ability of the ER to take up Ca^{2+}, and therefore these data could indicate that edelfosine affects one of the major functions of the ER, by altering the ER calcium level in a time-dependent way, which could have consequences in the cell's fate. Thus, edelfosine affects a number of ER-related processes and functions.

Involvement of caspases 8 and 10, and cleavage of Bid in edelfosine-induced apoptosis

BAP31 cleavage by edelfosine (Figure 2b) suggested the involvement of caspase-8 in the process. Western blot analyses showed early cleavage of procaspases 8 and 10 in pancreatic cancer cells after edelfosine treatment, as assessed by the appearance of p18 active caspase-8 and p23 active caspase-10 forms (Figure 4a). Preincubation of cells with caspase-8 inhibitor z-IETD-fmk and caspase-10 inhibitor z-AEVD-fmk blocked edelfosine-induced apoptosis (Figure 4b). Thus, both caspases 8 and 10 are involved in the apoptosis response induced by edelfosine in pancreatic cancer cells.

Bid is a potent proapoptotic Bcl-2 family member which, upon proteolytic activation by caspases 8 or 10, translocates onto mitochondria to promote activation of the Bax/Bak subgroup of the apoptotic Bcl-2 family proteins, and thereby contributes to the release of cytochrome *c* (Kuwana et al., 2005). We found Bid cleavage after edelfosine treatment, by using an anti-Bid antibody that recognizes both full-length and 18-kDa cleaved forms (Figure 4c). These results suggested that Bid might play a role in edelfosine-induced apoptosis by transferring signals to mitochondria.

Involvement of mitochondria in edelfosine-induced apoptosis in human pancreatic cancer cells

Because the above results showed that edelfosine promoted the cleavage of BAP31 and Bid into p20 and p18 fragments, acting as transmitters towards mitochondria in apoptosis signaling, we next analyzed the role of mitochondria in the apoptotic response triggered by edelfosine in pancreatic cancer cells. Once cytochrome *c* is released from mitochondria to the cytosol during apoptosis, it leads to formation of the apoptotic protease-activating factor-1 (Apaf-1)/Caspase-9 complex, initiating an apoptotic protease cascade that promotes degradation of key structural proteins, including poly(ADP-ribose) polymerase (PARP), causing DNA fragmentation and apoptosis. We found that edelfosine induced caspase-9, -7 and -3 activation, assessed by cleavage of procaspase-9, -7, and -3 into their respective active forms, as well as proteolysis of the caspase-3 and caspase-7 substrate poly(ADP-ribose) polymerase (PARP) in all pancreatic cancer cells assayed (Figure 5a). The caspase-9 inhibitor z-LEHD-fmk, and the caspase-3 inhibitor Ac-DEVD-CHO, inhibited the apoptotic death of pancreatic cancer cells induced by edelfosine (Figure 5b). In addition, inhibition of caspases by the broad caspase inhibitor z-VAD-fmk completely abrogated edelfosine-induced apoptosis (Figure 5b). These findings indicate that edelfosine-induced apoptosis in human pancreatic cancer cells is caspase-dependent.

As shown in Figure 5c, edelfosine treatment induced a marked release of cytochrome *c* from the mitochondria to the cytosol in BxPC-3 pancreatic cancer cells. Similarly, we also found mitochondrial cytochrome *c* release in Capan-2, CFPAC-1 and HuP-T4 pancreatic cancer cells following edelfosine treatment (Supplementary Figure S2). Because Bcl-x_L acts as a safeguard of mitochondria, preventing cytochrome *c* release and apoptosis, we stably transfected BxPC-3 cells with pSFFV-*bcl*-x_L plasmid (BxPC-3-Bcl-X_L), containing the human *bcl*-x_L open reading frame, or with control pSFFV-Neo plasmid (BxPC-3-Neo). BxPC-3-Neo cells behaved similarly as non-transfected BxPC-3 cells regarding all parameters studied. BxPC-3-Neo cells expressed a small level of endogenous Bcl-X_L, whereas a high expression of this protein was observed in BxPC-3-Bcl-X_L cells (Figure 5d). While BxPC-3-Neo cells underwent apoptosis after treatment with edelfosine, Bcl-X_L overexpression prevented edelfosine-induced apoptosis (Figure 5e). Edelfosine induced mitochondrial release of cytochrome *c* in BxPC-3-Neo cells (Figure 5f), but cytochrome *c* release was highly diminished in BxPC-3-Bcl-X_L cells (Figure 5f). These data show that mitochondria are involved in edelfosine-induced pancreatic cancer cell death.

In vivo antitumor effect of edelfosine in a pancreatic cancer xenograft model

We next evaluated the effect of orally administered edelfosine in two pancreatic cancer xenograft animal models. Following toxicity analyses with CB17-severe combined immunodeficient (CB17-SCID) and BALB/c mice (data not shown), we found that a daily oral administration dose of 30 mg/kg edelfosine was well tolerated, 45 mg/kg being the maximum tolerated dose. CB17-SCID mice were inoculated with 5 x 10^6 Capan-2 or HuP-T4 cells. When appreciable tumors were observed in the two pancreatic cancer animal models, mice were randomly assigned to cohorts of 8 mice each, receiving a daily oral administration of edelfosine (30 mg/kg) or an equal volume of vehicle (water). Serial caliper measurements were done every 3 days to calculate tumor volume until mice were sacrificed (Figure 6a). A comparison of tumors isolated from untreated control and drug-treated Capan-2 or HuP-T4-bearing mice, at the end of the treatment, rendered a remarkable anti-pancreatic cancer activity of edelfosine (Figure 6, b and c), with a statistically significant ($P < 0.05$) reduction of ~57% and ~66% in the tumor weight in both Capan-2 (233 ± 50 mg *vs*. 539 ± 106 mg, for edelfosine-treated *vs.* untreated mice, $n = 8$) and HuP-T4 (305 ± 67 mg *vs*. 896 ± 97 mg, for edelfosine-treated *vs.* untreated mice, $n = 8$) animal models (Figure 6b). Likewise, a statistically significant ($P < 0.05$) reduction of ~60% and ~72 % in tumor volume was also detected in both Capan-2 (240 ± 48 mm^3 *vs*. 600 ± 124 mm^3, for edelfosine-treated *vs.* untreated mice, *n* = 8) and HuP-T4 (312 ± 68 mm^3 *vs.* 1114 ± 145 mm^3, for edelfosine-treated *vs.* untreated mice, *n* = 8) animal models (Figure 6b). Interestingly, while tumors from drug-free mice showed a highly vascular appearance, tumors from edelfosine-treated mice were pale and poorly vascularized (Figure 6c). Organ examination at necropsy did not reveal any apparent toxicity (data not shown), and no significant differences in mean body weight were detected between drug-treated and drug-free control animals (2-3% of body weight loss in the drug-treated *vs.* drug-free control groups).

In vivo identification of apoptosis and ER stress in pancreatic tumors following edelfosine oral treatment

Histological patterns of tumors isolated from control drug-free tumor-bearing animals revealed a relative uniformity in cell size and morphology (Figure 7a). In contrast, examination of hematoxylin and eosin (H&E)-stained sections of tumors from mice orally treated with edelfosine showed the presence of irregular, large and medium-sized giant cells with eosinophilic cytoplasm. The nuclei in dying cells were either pyknotic or displayed nuclear fragmentation characteristic of cell death by apoptosis (Figure 7a). Induction of apoptosis was further supported by performing TUNEL apoptosis assay in tumor sections. No TUNEL fluorescence intensity expression was found in the tumor xenografts of the control drug-free group (Figure 7b). However, a strong TUNEL-positive signal, indicating apoptotic cells, was detected in the edelfosine-treated group (Figure 7b). Our data showed a significant difference in the percentage of TUNEL-positive cells between control drug-free and drug-treated groups, namely 2.2 ± 0.6 % *vs*. 35.0 ± 5.4 %.

The anti-activated caspase-3 specific antibody selectively labeled the cytoplasm of cells that had a morphology consistent with apoptosis in tumors from drug-treated mice (Figure 7c), while lack of staining was observed in control drug-free group. Our data showed that the caspase-3 labeling index in the tumor tissue of the drug-treated mice was significantly higher (40 ± 5.6 %) than that in the drug-free mice (1.2 ± 0.1 %) (Figure 7c).

Interestingly, the ER stress-associated marker CHOP/GADD153 was visualized by immunohistochemistry in the nuclei of cells in the pancreatic tumor isolated from edelfosine-treated mice, indicating a strong ER stress response in the tumor sections. However, CHOP/GADD153 staining was absent in tumors derived from control drug-free mice (Figure 7d).

Discussion

Pancreatic adenocarcinoma responds poorly to current therapies and remains as an incurable malignancy. This makes this tumor especially challenging for searching novel effective anticancer drugs. Our *in vitro* and *in vivo* data indicate that edelfosine is a potent antitumor agent against pancreatic tumor cells, and highlight the importance of ER as a target for the treatment of pancreatic cancer. We have found that edelfosine behaves as the most potent ALP in killing human pancreatic cancer cells by targeting ER. Perifosine was also active against pancreatic cancer cells, but other ALPs, such as miltefosine and erucylphosphocholine, as well as the structurally related inactive molecule ET-18-OH, failed to induce death cell in these cells, underlining the importance of the molecular structure of edelfosine for its anti-pancreatic cancer activity. The studies reported here show for the first time *in vitro* and *in vivo* evidences for the induction of ER stress in the mechanism of action of an ER-targeted antitumor drug in pancreatic cancer, suggesting that this could be a promising therapeutic approach in the treatment of pancreatic cancer.

We have found evidence that edelfosine was working *in vivo* in a similar manner to that observed *in vitro*. Oral administration of edelfosine showed a remarkable *in vivo* antitumor and proapoptotic activity, promoting a potent apoptosis response in human tumor xenografts in SCID mice, as assessed by morphological changes, TUNEL assay and caspase-3 activation. Our present data represent the first demonstration of the *in* *vivo* proapoptotic activity of edelfosine, which further support the notion that the antitumor action of this ALP highly depends on its ability to promote apoptosis in tumors. Edelfosine treatment led to dramatic tumor regression in pancreatic tumor animal models, and tumors became smaller and poorly vascularized, which could be in agreement with reports showing an antiangiogenic effect of edelfosine (Zerp *et al.*, 2008).

Pancreatic cancer cells have been reported to show prominent ER (Klimstra *et al.*, 1992; Skarda *et al.*, 1994). Here, we report for the first time that edelfosine accumulates in the ER of human pancreatic cancer cells and triggers a prolonged ER stress response, leading to apoptosis. Unlike several anticancer drugs that induce ER stress in an indirect way, here we found that edelfosine accumulates in the ER of human pancreatic cancer cells, and promotes a number of changes in ER-regulated homeostatic processes, leading to the triggering of sundry ER-derived apoptotic events that eventually converge on the mitochondria. Edelfosine also upregulates *sXbp1*, a key modulator of the UPR, but activation of this protective response during ER stress seems not to be enough to prevent apoptosis. The role of UPR activation in edelfosine-induced apoptosis remains to be elucidated, and we cannot rule out that upregulation of the above UPR marker might merely be a correlative phenomenon. The results obtained measuring the effects of edelfosine on $[Ca^{2+}]_{ER}$ in BxPc-3 cells suggest that edelfosine induces a significant deregulation of global Ca^{2+} homeostasis. We have previously shown that edelfosine increases cytosolic $[Ca^{2+}]$ in HeLa cells (Nieto-Miguel *et al.*, 2007). On these grounds, and taking into account the interaction of edelfosine with cell membranes and lipids (Ausili *et al.*, 2008; Busto *et al.*, 2008; Busto *et al.*, 2007; Gajate *et al.*, 2004; Gajate *et al.*, 2009a; Gajate *et al.*, 2009b; Mollinedo *et al.*, 2010; Mollinedo and Gajate, 2006; Torrecillas *et al.*, 2006; Zaremberg *et al.*, 2005), it might be envisaged that the increase in cytosolic $[Ca^{2+}]$ could be due to an increased permeability of the plasma membrane, resulting in Ca^{2+} entry from the extracellular medium, which it then leads to the herein reported increase in $[Ca^{2+}]_{ER,}$ well above the steady state levels in control cells. The effect on $[Ca^{2+}]_{ER}$ may seem puzzling, because ER stress has been rather associated with ER-stored Ca^{2+} release. However, our present results also indicate that this Ca^{2+} pumping into the ER, following edelfosine incubation, is progressively decreased with time. These results might reflect an altered function of the ER, leading to a gradual impairment in its capacity to take up Ca^{2+}, and hence to Ca^{2+} homeostasis deregulation in the ER. All these aspects deserve further studies on the role of Ca^{2+} in the proapoptotic action of edelfosine in pancreatic cancer cells.

Figure 8 depicts a model for the involvement of ER in edelfosine-induced apoptosis in pancreatic cancer cells. Our previous (Nieto-Miguel *et al.*, 2007) and present data suggest that edelfosine causes a gradual alteration in calcium homeostasis. Transient increase in cytosolic Ca^{2+} stimulates Ca^{2+} uptake by mitochondria (Rizzuto and Pozzan, 2006), which contributes to mitochondrial membrane permeability transition, releasing apoptogenic proteins. Here, we have found that edelfosine induces cytochrome *c* release from mitochondria in pancreatic cancer cells. Cytochrome *c* released from mitochondria binds to Apaf-1 and procaspase-9 to form the so-called apoptosome (Riedl and Salvesen, 2007). This complex catalyzes the activation of caspases that executes the apoptotic cell death program. The herein reported abrogation of edelfosine-induced apoptosis, and mitochondrial cytochrome *c* release, by Bcl-X_L overexpression indicates an essential role for mitochondria in the induction of apoptosis by this anticancer drug in pancreatic cancer cells. ER stress-induced processing of procaspase-9 can also occur in the absence of cytochrome *c* release and in Apaf-1-null fibroblasts (Rao *et al.*, 2002), suggesting that caspase-4 can directly trigger caspase-9 activation and apoptosis independently of the mitochondrial cytochrome *c*/Apaf-1 pathway, at least in certain cell types. Our results suggest that both caspase-4- and apoptosome-mediated signaling pathways are involved in edelfosine-induced apoptosis (Figure 8). A prolonged ER stress during exposure to edelfosine leads to the induction of a proapoptotic transcription factor, CHOP/GADD153. Here, we found both *in vitro* and *in vivo* evidence for the upregulation of CHOP/GADD153 following edelfosine treatment in pancreatic cancer cells, whereas the level of GRP78/BiP protein was not significantly altered, tipping the balance in favor of an ER stress-induced cell death. Thus, these results imply that induction of CHOP/GADD153 expression is closely associated with the progression of apoptosis during exposure of pancreatic cancer cells to edelfosine. Our data suggest that edelfosine induces in pancreatic cancer cells the cleavage of BAP31, an integral membrane protein of the ER, with the formation of p20 fragment that directs proapoptotic signals between ER and mitochondria, resulting in the discharge of Ca^{2+} from the ER and its concomitant uptake into the mitochondria. Also, edelfosine promotes phosphorylation of eIF2α, another typical response to ER stress. In addition, we found that ER stress-associated caspase-4 was activated before the onset of apoptosis following edelfosine treatment in pancreatic cancer cells. Caspase-4 inhibition abrogated edelfosine-induced apoptosis, suggesting that caspase-4 is required for the triggering of cell death. In addition, edelfosine-induced apoptosis in pancreatic cancer cells involves caspase-8 activation and persistent activation of JNK.

Members of the Bcl-2 family are also involved in the regulation of cell death induced by ER stress (Oakes *et al.*, 2006). In normal conditions, mammalian cells express low levels of Bax, which is predominantly a soluble monomeric protein in the cytosol (Hsu *et al.*, 1997). Under ER stress conditions, a significant fraction of Bax may translocate from cytosol to membrane fractions, in particular the mitochondrial membrane (Hsu *et al.*, 1997). Insertion of Bax into mitochondria causes the release of cytochrome *c* and Ca^{2+} to the cytosol. Our previous (Mollinedo *et al.*, 1997; Nieto-Miguel *et al.*, 2007) and present data indicate that edelfosine does not modify the expression of antiapoptotic Bcl-2 and Bcl-X_L genes, whereas Bax is activated. In addition, cells lacking both Bax and Bak have been shown resistant to ER stress-induced apoptosis (Zong *et al.*, 2001). We have previously reported that $bax^{-/-}/bak^{-/-}$ double-knockout cells fail to undergo edelfosine-induced ER-stored Ca^{2+} release and apoptosis (Nieto-Miguel *et al.*, 2007). Taken together, our previous and present results suggest a role for Bax in edelfosine-induced apoptosis in pancreatic cancer cells.

Overall, the results reported here indicate that edelfosine exerts its proapoptotic action in pancreatic cancer cells, both *in vitro* and *in vivo*, through its accumulation in the ER that leads to a sustained ER stress, and eventually to cell death. These data suggest that ER targeting by edelfosine may represent a promising new framework in the treatment of currently incurable pancreatic cancer. Our results also provide a rationale for searching new effective agents targeting ER to treat pancreatic cancer.

Materials and methods

Reagents

Detailed information on the reagents used is included in Supplementary data.

Cell culture

Detailed information on the cell lines used is included in Supplementary data.

bcl-x_L transfection

BxPC-3 cells (1-2 X 10^5) were transfected with 8 µg of pSFFV-Neo or pSFFV-*bcl-x_L* expression vector as previously described (Mollinedo *et al.*, 1997), using Lipofectin reagent (Life Technologies, Carlsbad, CA). Transfected clones were selected by growth in the presence of 600 µg/ml of G418 (Sigma), and then cultured at 250 µg/ml of G418, and monitored by Western blotting using the 2H12 anti-29 kDa Bcl-X_L monoclonal antibody (BD Biosciences Pharmingen, San Diego, CA).

Edelfosine uptake

Drug uptake was measured as previously described (Mollinedo *et al.*, 1997) with slight modifications. After incubating 10^6/ml cells with 10 µM edelfosine plus 0.05 µCi/ml [^{3}H]edelfosine for 1 h, and subsequent exhaustive washing (five times) with 1% BSA-

PBS, 0.1 ml of 0.2% Triton X-100 was added to the cell pellets, and the incorporated radioactivity was counted on a beta-counter by mixing with water-miscible liquid scintillation cocktail. [^{3}H]edelfosine (specific activity, 42 Ci/mmol) was synthesized by tritiation of the 9-octadecenyl derivative (Amersham Buchler, Braunschweig, Germany).

Drug subcellular localization

The subcellular localization of edelfosine in pancreatic cancer cells was examined with the newly synthesized edelfosine fluorescent analog 1-*O*-[11'-(6''-ethyl-1'',3'',5'',7''-tetramethyl-4'',4''-difluoro-4''-bora-3a'',4a''-diaza-*s*-indacen-2''-yl)undecyl]-2-*O*-methyl-*rac*-glycero-3-phosphocholine (Et-BDP-ET) (Mollinedo *et al.*, 2011), a kind gift from F. Amat-Guerri and A. U. Acuña (Consejo Superior de Investigaciones Científicas, Madrid, Spain). ER was visualized by transfecting cells with 4 µg of a plasmid encoding endoplasmic reticulum-targeted red fluorescence protein (erRFP) (Klee and Pimentel-Muinos, 2005), kindly provided by F. X. Pimentel-Muinos (Instituto de Biología Molecular y Celular del Cáncer, Centro de Investigación del Cáncer, Salamanca, Spain). Detailed information on the conditions used in this study is included in Supplementary data.

Apoptosis assay

Quantitation of apoptotic cells was determined by flow cytometry as the percentage of cells in the sub-G_1 region (hypodiploidy) in cell cycle analysis as previously described (Gajate *et al.*, 2000b).

$[Ca^{2+}]_{ER}$ measurements with aequorin

BxPc-3 cells were transiently transfected with ER-targeted mutated aequorin (Alvarez and Montero, 2002; Montero *et al.*, 1997a). The cells were plated onto 13-mm round coverslips. Before reconstituting aequorin, $[Ca^{2+}]_{ER}$ was reduced by incubating the cells for 5-10 min at room temperature with the sarcoplasmic and endoplasmic reticulum

Ca^{2+}-ATPase inhibitor 2,5-di-tert-buthyl-benzohydroquinone (BHQ) (10 μM) in standard external medium containing: 145 mM NaCl, 5 mM KCl, 1 mM $MgCl_2$, 10 mM glucose, 10 mM HEPES, pH 7.4, supplemented with 3 mM EGTA. Cells were then incubated for 90 min at room temperature in standard medium containing 0.5 mM EGTA, 10 μM BHQ and 2 μM coelenterazine n. The coverslip was then placed in the perfusion chamber of a purpose-built thermostatized luminometer, and standard medium containing 1 mM Ca^{2+} was perfused to refill the ER with Ca^{2+}. Calibration of the luminescence data into $[Ca^{2+}]$ was made using an algorithm as previously described (Alvarez and Montero, 2002).

Western blot

Cells (4-5 X 10^6) were lysed with 60 μl of 25 mM Hepes (pH 7.7), 0.3 M NaCl, 1.5 mM $MgCl_2$, 0.2 mM EDTA, 0.1 % Triton X-100, 20 mM β-glycerophosphate, 0.1 mM sodium orthovanadate, supplemented with protease inhibitors (1 mM phenylmethylsulfonyl fluoride, 20 μg/ml aprotinin, 20 μg/ml leupeptin). Proteins (45 μg) were run on SDS-polyacrylamide gels, transferred to nitrocellulose filters, blocked with 5% (w/v) defatted powder milk in 50 mM Tris-HCl (pH 8.0), 150 mM NaCl, and 0.1% Tween 20 (TBST) for 60 min at room temperature, and then incubated for 1 h at room temperature or overnight at 4ºC with specific antibodies. Detailed information on the antibodies used is included in Supplementary data.

Mitochondrial cytochrome c release measurement

Release of cytochrome *c* from mitochondria to cytosol was analyzed by Western blot as previously described (Gajate and Mollinedo, 2001; Pique *et al.*, 2000).

Solid phase JNK assay

Protein kinase assays were carried out using a fusion protein between glutathione S-transferase and c-Jun (amino acids 1-223) as a substrate of JNK, as previously described (Gajate *et al.*, 2000a; Gajate *et al.*, 1998).

Reverse transcriptase-polymerase chain reaction (RT-PCR) and restriction analysis

Detailed information on the conditions for RT-PCR and primer sequences are included in Supplementary data. Subsequent *Pst*I restriction analysis of the *XBP1* amplicon was carried out following standard procedures.

Xenograft mouse models

Eight-week-old female CB17-SCID mice (Charles River Laboratories, Lyon, France), kept and handled according to institutional guidelines, complying with Spanish legislation under 12/12 h light/dark cycle at a temperature of 22ºC, received a standard diet and acidified water *ad libitum*. Capan-2 and HuP-T4 cells (5×10^6) were injected subcutaneously in 100 μl PBS together with 100 μl Matrigel basement membrane matrix (Becton Dickinson, Franklin Lakes, NJ) into the right flank of each mouse. When tumors were palpable, approximately 2 weeks after tumor cell implantation, mice were randomly assigned to cohorts of 8 mice each, receiving a daily oral administration of edelfosine (30 mg/kg of body weight) or an equal volume of vehicle (water). The shortest and longest diameter of the tumor were measured with calipers at the indicated time intervals, and tumor volume (mm^3) was calculated using the following standard formula: (the shortest diameter)^2 x (the longest diameter) x 0.5. Animal body weight and any sign of morbidity were monitored. Drug treatment lasted 32 days for Capan-2-bearing mice, and 47 days for HuP-T4-bearing mice. Animals were killed 24 h after the last drug administration according to institutional guidelines, and tumors were carefully removed, weighed, and analyzed. A necropsy analysis involving tumors and distinct organs was carried out.

TUNEL assay in tumor sections

The DeadEnd^{TM} Fluorometric TUNEL System (Promega, Madison, WI) was used to detect apoptosis. Detailed information on the conditions used in this study is included in Supplementary data.

Immunohistochemistry

Tumor tissue samples were fixed in 4% buffered paraformaldehyde and embedded in paraffin. Detailed information on the conditions used in this study is included in Supplementary data.

Statistical analysis

The results given are the mean ± standard deviation (SD) of the number of experiments indicated. Statistical evaluation was performed by Student's *t*-test. A *P*-value of < 0.05 was considered statistically significant.

Conflict of interest

The authors declare no conflict of interest

Acknowledgements

This work was supported by grants from Fondo de Investigación Sanitaria and European Commission (FIS-FEDER PS09/01915), Ministerio de Ciencia e Innovación (SAF2008-02251, BFU 2008-01871, and RD06/0020/1037 from Red Temática de Investigación Cooperativa en Cáncer, Instituto de Salud Carlos III), European Community's Seventh Framework Programme FP7-2007-2013 (grant HEALTH-F2-2011-256986), and Junta de Castilla y León (CSI052A11-2, GR15-Experimental Therapeutics and Translational Oncology Program, Biomedicine Project 2009, and Biomedicine Project 2010-2011). C.G. is supported by the Ramón y Cajal Program from the Ministerio de Ciencia e Innovación of Spain.

References

Alvarez J, Montero M. (2002). Measuring [Ca^{2+}] in the endoplasmic reticulum with aequorin. *Cell Calcium* **32:** 251-260.

Ausili A, Torrecillas A, Aranda FJ, Mollinedo F, Gajate C, Corbalan-Garcia S *et al.* (2008). Edelfosine is incorporated into rafts and alters their organization. *J Phys Chem B* **112:** 11643-11654.

Breckenridge DG, Stojanovic M, Marcellus RC, Shore GC. (2003). Caspase cleavage product of BAP31 induces mitochondrial fission through endoplasmic reticulum calcium signals, enhancing cytochrome c release to the cytosol. *J Cell Biol* **160:** 1115-1127.

Busto JV, Del Canto-Janez E, Goni FM, Mollinedo F, Alonso A. (2008). Combination of the anti-tumour cell ether lipid edelfosine with sterols abolishes haemolytic side effects of the drug. *J Chem Biol* **1:** 89-94.

Busto JV, Sot J, Goni FM, Mollinedo F, Alonso A. (2007). Surface-active properties of the antitumour ether lipid 1-*O*-octadecyl-2-*O*-methyl-*rac*-glycero-3-phosphocholine (edelfosine). *Biochim Biophys Acta* **1768:** 1855-1860.

Carracedo A, Gironella M, Lorente M, Garcia S, Guzman M, Velasco G *et al.* (2006). Cannabinoids induce apoptosis of pancreatic tumor cells via endoplasmic reticulum stress-related genes. *Cancer Res* **66:** 6748-6755.

Cunha DA, Hekerman P, Ladriere L, Bazarra-Castro A, Ortis F, Wakeham MC *et al.* (2008). Initiation and execution of lipotoxic ER stress in pancreatic beta-cells. *J Cell Sci* **121:** 2308-2318.

Estella-Hermoso de Mendoza A, Campanero MA, de la Iglesia-Vicente J, Gajate C, Mollinedo F, Blanco-Prieto MJ. (2009). Antitumor alkyl ether lipid edelfosine: tissue distribution and pharmacokinetic behavior in healthy and tumor-bearing immunosuppressed mice. *Clin Cancer Res* **15:** 858-864.

Fonseca SG, Burcin M, Gromada J, Urano F. (2009). Endoplasmic reticulum stress in beta-cells and development of diabetes. *Curr Opin Pharmacol* **9:** 763-770.

Fribley A, Zeng Q, Wang CY. (2004). Proteasome inhibitor PS-341 induces apoptosis through induction of endoplasmic reticulum stress-reactive oxygen species in head and neck squamous cell carcinoma cells. *Mol Cell Biol* **24:** 9695-9704.

Gajate C, Barasoain I, Andreu JM, Mollinedo F. (2000a). Induction of apoptosis in leukemic cells by the reversible microtubule-disrupting agent 2-methoxy-5-(2',3',4'-trimethoxyphenyl)-2,4,6-cycloheptatrien-1-one: protection by Bcl-2 and Bcl-X_L and cell cycle arrest. *Cancer Res* **60:** 2651-2659.

Gajate C, Del Canto-Janez E, Acuna AU, Amat-Guerri F, Geijo E, Santos-Beneit AM *et al.* (2004). Intracellular triggering of Fas aggregation and recruitment of apoptotic molecules into Fas-enriched rafts in selective tumor cell apoptosis. *J Exp Med* **200:** 353-365.

Gajate C, Fonteriz RI, Cabaner C, Alvarez-Noves G, Alvarez-Rodriguez Y, Modolell M *et al.* (2000b). Intracellular triggering of Fas, independently of FasL, as a new mechanism of antitumor ether lipid-induced apoptosis. *Int J Cancer* **85:** 674-682.

Gajate C, Gonzalez-Camacho F, Mollinedo F. (2009a). Involvement of raft aggregates enriched in Fas/CD95 death-inducing signaling complex in the antileukemic action of edelfosine in Jurkat cells. *PLoS One* **4:** e5044.

Gajate C, Gonzalez-Camacho F, Mollinedo F. (2009b). Lipid raft connection between extrinsic and intrinsic apoptotic pathways. *Biochem Biophys Res Commun* **380:** 780-784.

Gajate C, Mollinedo F. (2001). The antitumor ether lipid ET-18-OCH_3 induces apoptosis through translocation and capping of Fas/CD95 into membrane rafts in human leukemic cells. *Blood* **98:** 3860-3863.

Gajate C, Mollinedo F. (2002). Biological activities, mechanisms of action and biomedical prospect of the antitumor ether phospholipid ET-18-OCH_3 (edelfosine), a proapoptotic agent in tumor cells. *Curr Drug Metab* **3:** 491-525.

Gajate C, Mollinedo F. (2007). Edelfosine and perifosine induce selective apoptosis in multiple myeloma by recruitment of death receptors and downstream signaling molecules into lipid rafts. *Blood* **109:** 711-719.

Gajate C, Santos-Beneit A, Modolell M, Mollinedo F. (1998). Involvement of c-Jun NH_2-terminal kinase activation and c-Jun in the induction of apoptosis by the ether phospholipid 1-*O*-octadecyl-2-*O*-methyl-*rac*-glycero-3-phosphocholine. *Mol Pharmacol* **53:** 602-612.

Hirota M, Kitagaki M, Itagaki H, Aiba S. (2006). Quantitative measurement of spliced XBP1 mRNA as an indicator of endoplasmic reticulum stress. *J Toxicol Sci* **31:** 149-156.

Hitomi J, Katayama T, Eguchi Y, Kudo T, Taniguchi M, Koyama Y *et al.* (2004). Involvement of caspase-4 in endoplasmic reticulum stress-induced apoptosis and Abeta-induced cell death. *J Cell Biol* **165:** 347-356.

Hsu YT, Wolter KG, Youle RJ. (1997). Cytosol-to-membrane redistribution of Bax and Bcl-X_L during apoptosis. *Proc Natl Acad Sci U S A* **94:** 3668-3672.

Jemal A, Siegel R, Ward E, Murray T, Xu J, Thun MJ. (2007). Cancer statistics, 2007. *CA Cancer J Clin* **57:** 43-66.

Klee M, Pimentel-Muinos FX. (2005). Bcl-X_L specifically activates Bak to induce swelling and restructuring of the endoplasmic reticulum. *J Cell Biol* **168:** 723-734.

Klimstra DS, Heffess CS, Oertel JE, Rosai J. (1992). Acinar cell carcinoma of the pancreas. A clinicopathologic study of 28 cases. *Am J Surg Pathol* **16:** 815-837.

Kuwana T, Bouchier-Hayes L, Chipuk JE, Bonzon C, Sullivan BA, Green DR *et al.* (2005). BH3 domains of BH3-only proteins differentially regulate Bax-mediated mitochondrial membrane permeabilization both directly and indirectly. *Mol Cell* **17:** 525-535.

Li D, Xie K, Wolff R, Abbruzzese JL. (2004). Pancreatic cancer. *Lancet* **363:** 1049-1057.

Li J, Lee AS. (2006). Stress induction of GRP78/BiP and its role in cancer. *Curr Mol Med* **6:** 45-54.

Mandic A, Hansson J, Linder S, Shoshan MC. (2003). Cisplatin induces endoplasmic reticulum stress and nucleus-independent apoptotic signaling. *J Biol Chem* **278:** 9100-9106.

Mimnaugh EG, Xu W, Vos M, Yuan X, Isaacs JS, Bisht KS *et al.* (2004). Simultaneous inhibition of hsp 90 and the proteasome promotes protein ubiquitination, causes endoplasmic reticulum-derived cytosolic vacuolization, and enhances antitumor activity. *Mol Cancer Ther* **3:** 551-566.

Mollinedo F, de la Iglesia-Vicente J, Gajate C, Estella-Hermoso de Mendoza A, Villa-Pulgarin JA, Campanero MA *et al.* (2010). Lipid raft-targeted therapy in multiple myeloma. *Oncogene* **29:** 3748-3757.

Mollinedo F, Fernandez M, Hornillos V, Delgado J, Amat-Guerri F, Acuna AU *et al.* (2011). Involvement of lipid rafts in the localization and dysfunction effect of the antitumor ether phospholipid edelfosine in mitochondria. *Cell Death Dis* **2:** e158.

Mollinedo F, Fernandez-Luna JL, Gajate C, Martin-Martin B, Benito A, Martinez-Dalmau R *et al.* (1997). Selective induction of apoptosis in cancer cells by the ether lipid ET-18-OCH_3 (Edelfosine): molecular structure requirements, cellular uptake, and protection by Bcl-2 and Bcl-X_L. *Cancer Res* **57:** 1320-1328.

Mollinedo F, Gajate C. (2006). Fas/CD95 death receptor and lipid rafts: new targets for apoptosis-directed cancer therapy. *Drug Resist Updat* **9:** 51-73.

Mollinedo F, Gajate C. (2010). Lipid rafts and clusters of apoptotic signaling molecule-enriched rafts in cancer therapy. *Future Oncol* **6:** 811-821.

Mollinedo F, Gajate C, Martin-Santamaria S, Gago F. (2004). ET-18-OCH_3 (edelfosine): a selective antitumour lipid targeting apoptosis through intracellular activation of Fas/CD95 death receptor. *Curr Med Chem* **11:** 3163-3184.

Montero M, Alvarez J, Scheenen WJ, Rizzuto R, Meldolesi J, Pozzan T. (1997a). Ca^{2+} homeostasis in the endoplasmic reticulum: coexistence of high and low [Ca^{2+}] subcompartments in intact HeLa cells. *J Cell Biol* **139:** 601-611.

Montero M, Barrero MJ, Alvarez J. (1997b). [Ca^{2+}] microdomains control agonist-induced Ca^{2+} release in intact HeLa cells. *Faseb J* **11:** 881-885.

Neoptolemos JP, Cunningham D, Friess H, Bassi C, Stocken DD, Tait DM *et al.* (2003). Adjuvant therapy in pancreatic cancer: historical and current perspectives. *Ann Oncol* **14:** 675-692.

Nieto-Miguel T, Fonteriz RI, Vay L, Gajate C, Lopez-Hernandez S, Mollinedo F. (2007). Endoplasmic reticulum stress in the proapoptotic action of edelfosine in solid tumor cells. *Cancer Res* **67:** 10368-10378.

Nishitoh H, Matsuzawa A, Tobiume K, Saegusa K, Takeda K, Inoue K *et al.* (2002). ASK1 is essential for endoplasmic reticulum stress-induced neuronal cell death triggered by expanded polyglutamine repeats. *Genes Dev* **16:** 1345-1355.

Oakes SA, Lin SS, Bassik MC. (2006). The control of endoplasmic reticulum-initiated apoptosis by the BCL-2 family of proteins. *Curr Mol Med* **6:** 99-109.

Oyadomari S, Araki E, Mori M. (2002). Endoplasmic reticulum stress-mediated apoptosis in pancreatic beta-cells. *Apoptosis* **7:** 335-345.

Oyadomari S, Mori M. (2004). Roles of CHOP/GADD153 in endoplasmic reticulum stress. *Cell Death Differ* **11:** 381-389.

Pique M, Barragan M, Dalmau M, Bellosillo B, Pons G, Gil J. (2000). Aspirin induces apoptosis through mitochondrial cytochrome c release. *FEBS Lett* **480:** 193-196.

Rao RV, Castro-Obregon S, Frankowski H, Schuler M, Stoka V, del Rio G *et al.* (2002). Coupling endoplasmic reticulum stress to the cell death program. An Apaf-1-independent intrinsic pathway. *J Biol Chem* **277:** 21836-21842.

Riedl SJ, Salvesen GS. (2007). The apoptosome: signalling platform of cell death. *Nat Rev Mol Cell Biol* **8:** 405-413.

Rizzuto R, Pozzan T. (2006). Microdomains of intracellular $Ca2^{+}$: molecular determinants and functional consequences. *Physiol Rev* **86:** 369-408.

Ron D, Habener JF. (1992). CHOP, a novel developmentally regulated nuclear protein that dimerizes with transcription factors C/EBP and LAP and functions as a dominant-negative inhibitor of gene transcription. *Genes Dev* **6:** 439-453.

Skarda JS, Honick AB, Gibbins CS, Josselson AR, Rishi M. (1994). Papillary-cystic tumor of the pancreas in a young woman: fine-needle aspiration cytology, ultrastructure and DNA analysis. *Diagn Cytopathol* **10:** 20-24.

Torrecillas A, Aroca-Aguilar JD, Aranda FJ, Gajate C, Mollinedo F, Corbalan-Garcia S *et al.* (2006). Effects of the anti-neoplastic agent ET-18-OCH_3 and some analogs on the biophysical properties of model membranes. *Int J Pharm* **318:** 28-40.

Urano F, Wang X, Bertolotti A, Zhang Y, Chung P, Harding HP *et al.* (2000). Coupling of stress in the ER to activation of JNK protein kinases by transmembrane protein kinase IRE1. *Science* **287:** 664-666.

van Riel JM, van Groeningen CJ, Pinedo HM, Giaccone G. (1999). Current chemotherapeutic possibilities in pancreaticobiliary cancer. *Ann Oncol* **10 Suppl 4:** 157-161.

Zaremberg V, Gajate C, Cacharro LM, Mollinedo F, McMaster CR. (2005). Cytotoxicity of an anti-cancer lysophospholipid through selective modification of lipid raft composition. *J Biol Chem* **280:** 38047-38058.

Zerp SF, Vink SR, Ruiter GA, Koolwijk P, Peters E, van der Luit AH *et al.* (2008). Alkylphospholipids inhibit capillary-like endothelial tube formation *in vitro*:

antiangiogenic properties of a new class of antitumor agents*. Anticancer Drugs* **19:** 65-75.

Zong WX, Li C, Hatzivassiliou G, Lindsten T, Yu QC, Yuan J *et al.* (2003). Bax and Bak can localize to the endoplasmic reticulum to initiate apoptosis*. J Cell Biol* **162:** 59-69.

Zong WX, Lindsten T, Ross AJ, MacGregor GR, Thompson CB. (2001). BH3-only proteins that bind pro-survival Bcl-2 family members fail to induce apoptosis in the absence of Bax and Bak*. Genes Dev* **15:** 1481-1486.

Figure legends

Figure 1 Induction of apoptosis by edelfosine and structurally related compounds, and edelfosine uptake, in human pancreatic cancer cell lines. (**a**) Cells were incubated in the absence (Control) or in the presence of 10-20 μM edelfosine (EDLF) for the indicated times, and apoptosis was analyzed. (**b**) Cells untreated (Control) or treated with different alkyl-lysophospholipid analogues (20 μM) for the indicated times, were analyzed for apoptosis. (**c**) EDLF uptake in different pancreatic cancer cells. 10^6 cells/ml were incubated with 10 μM edelfosine + 0.05 μCi/ml [^{3}H]edelfosine for 1 h, and then cells were exhaustively washed (five times) with 1% BSA-PBS to remove the drug loosely bound to the external side of the cell membrane, and edelfosine uptake was determined by measuring incorporated radioactivity. Data shown are means ± SD of three independent experiments.

Figure 2 ER drug localization and ER stress in edelfosine-treated pancreatic tumor cells. (**a**) HuP-T4 and Capan-2 cells were transfected with erRFP plasmid to visualize ER (red fluorescence) and then incubated with Et-BDP-ET (green fluorescence). Cells were also stained for nuclei with DAPI (blue fluorescence). Areas of colocalization between ER and Et-BDP-ET in the merge panels are yellow. The corresponding differential interference contrast (DIC) microscopy images are also shown. (**b**) HuP-T4 cells, untreated (C) or treated with 20 μM edelfosine for the indicated times, were analyzed by Western blot using specific antibodies for the indicated proteins. β-Actin was used as a loading control. (**c**) Cells untreated (C) or treated with 20 μM EDLF for different times were analyzed for JNK activation. The migration position of GST-c-Jun-1-223 is indicated. Cells untreated (Control) or pre-treated with caspase-4 inhibitor z-LEVD-fmk (**d**) or JNK inhibitor SP600125 (BxPC-3 cells) (**e**) for 1 h, and then incubated without or with 20 μM EDLF for 48 h, were analyzed for apoptosis. (**f**) Cells were incubated without (C) or with edelfosine for the indicated times, and then total RNA was isolated and subjected to RT-PCR using specific primers for the *XBP1* gene. The positions of the amplification products *uXBP1* and *sXBP1* are indicated. PCR amplification of β-actin was used as an internal control. Data shown are means ± SD or representative experiments of three performed.

Figure 3 Edelfosine-mediated changes in $[Ca^{2+}]_{ER}$ in BxPC-3 cells. (**a**) Effect of edelfosine on ER calcium uptake. Cells were reconstituted with coelenterazine n, and then medium containing 1 mM Ca^{2+} was perfused as indicated. When a steady state was obtained, 10 μM edelfosine was added to the calcium containing medium. The trace shown is the mean of 5 different experiments. (**b**) Effect of preincubation with edelfosine on ER calcium refilling. Cells were reconstituted with coelenterazine n either in the presence of 10 μM edelfosine for the indicated times. Then 1 mM Ca^{2+} was perfused as indicated. Traces are the means of 7 (15 min), 3 (30 min) and 6 (60 min) different experiments.

Figure 4 Caspase-8/10 activation and Bid cleavage in edelfosine-treated pancreatic cancer cells. (**a**) Cells untreated (C) or treated with 20 μM edelfosine for the indicated times, were assayed for caspase-8 and caspase-10 activation by Western blot. (**b**) Cells untreated (Control) or pre-treated with caspase inhibitors z-IETD-fmk or z-AEVD-fmk for 1 h, and then incubated without or with 20 μM edelfosine (EDLF) for 48 h, were analyzed for apoptosis. (**c**) Time-course of Bid cleavage in cells untreated (C) or treated with 20 μM edelfosine. β-Actin was used as a loading control. Data shown are means ± SD or representative experiments of three performed.

Figure 5 Mitochondrial and caspase involvement in edelfosine-induced apoptosis in pancreatic cancer cells. (**a**) Cells were untreated (C) or treated with 20 μM edelfosine for the indicated times, and cleavage of caspase-9, -3, -7, and PARP was detected by Western blotting. β-Actin was used as a loading control. (**b**) Cells pre-incubated without (Control) or with caspase inhibitors z-LEHD-fmk, Ac-DEVD-CHO and z-VAD-fmk for 1 h, and then treated without or with 20 μM edelfosine (EDLF) for 48 h, were analyzed for apoptosis. (**c**) BxPC-3 cells were untreated (C) or treated with 20 μM edelfosine at the indicated times, and cytochrome *c* (Cyt *c*), β-actin, and cytochrome *c* oxidase subunit II (cyt c Ox. II) were analyzed in the cytosolic and mitochondrial fractions by Western blot. β-Actin and cytochrome *c* oxidase subunit II were used as controls for cytosolic and mitochondrial proteins, respectively, that do not relocate to other subcellular locations during treatment. (**d**) Cell lysates from Neo (*BxPC-3-Neo*) and Bcl-X_L (*BxPC-3-Bcl-X_L*) transfected BxPC-3 cells were subjected to immunoblotting and analyzed for the expression of Bcl-X_L protein. (**e**) BxPC-3-Neo and BxPC-3-Bcl-X_L cells were incubated for the indicated times without (Control) or with 20 μM edelfosine, and apoptosis was quantitated. (**f**) Western blot analysis of mitochondrial cytochrome *c* (Cyt *c*) release into the cytosolic fraction (CYT) in BxPC-3-Neo and BxPC-3-Bcl-X_L cells. Cytochrome *c* oxidase subunit II (cyt c Ox. II) in the mitochondrial fraction (MIT) was used as a control of the amount of mitochondria used in the experiment. Data shown are means ± SD or representative experiments of three performed.

Figure 6 Antitumor effect of edelfosine on human pancreatic cancer xenograft models. (**a**) CB17-SCID mice were inoculated subcutaneously with Capan-2 or HuP-T4 cells. Oral administration of edelfosine (30 mg/kg, once-daily dosing regimen) and water vehicle (Control) started after the development of a palpable tumor in tumor-bearing mice in parallel (n = 8). Caliper measurements of each tumor were carried out at the indicated times. Edelfosine (EDLF) inhibited significantly pancreatic tumor growth compared with the vehicle-treated control group ($P < 0.05$, between drug-treated and drug-free control mice; from days 9 and 18 of treatment in Capan-2- and HuP-T4-

bearing mice until the end of the experiments). Data shown in panel A are means ± SD (n = 8). (**b**) After completion of the *in vivo* assays, control and EDLF-treated mice were sacrificed and tumor weight and volume were measured. Average tumor size and weight values of each experimental group are shown. * indicates values that are statistically significant between drug-treated and drug-free control mice at $P < 0.05$. (**c**) A remarkable pancreatic tumor growth inhibition was observed after 32 and 47 days of edelfosine treatment in Capan-2- and HuP-T4-bearing SCID mice. Representative tumors isolated from drug-free pancreatic-bearing mice (Control) and drug-treated pancreatic tumor-bearing mice (EDLF) are shown.

Figure 7 Edelfosine induces apoptosis and CHOP/GADD153 expression in pancreatic xenograft tumor. (**a**) Microscopic view of the paraffin section of a human Capan-2 tumor xenograft stained with H&E from control drug-free and edelfosine-treated mice (400x magnification). Tissue sections of tumors from edelfosine-treated mice show the presence of irregular and medium-sized giant cells with eosinophilic cytoplasm (*arrow*), cells with pyknotic nuclei (*asterisk*), and apoptotic bodies characteristic of cell death by apoptosis (*arrowhead*). These alterations are not seen in the cancer cell morphology from drug-free control Capan-2 tumors. (**b**) Sections of Capan-2-bearing mice from control or edelfosine-treated were assayed for apoptosis by TUNEL staining. FITC-TUNEL reaction (*FITC*, green fluorescence) stains apoptotic nuclei. Propidium iodide (*PI*, red fluorescence) stains DNA in the whole cell population. Areas of colocalization between FITC-TUNEL and PI in the merge panels are yellow. The corresponding DIC microscopy images are also shown. (**c**) Treatment of Capan-2 tumor-bearing mice with edelfosine results in increased tumor apoptosis as detected by activated caspase-3 staining. Cleaved caspase-3-negative cells were shown in untreated mice (Control), whereas cleaved caspase-3-positive cells (arrows) were observed in edelfosine-treated mice. (**d**) Representative sections obtained from Capan-2-xenograft tumor tissues were stained for CHOP/GADD153. Positive staining is shown as dark blue coloring of the nucleus of the cells (arrows) in the edelfosine-treated tumor. Apoptotic cells, caspase-3 positive staining, and CHOP/GADD153 staining in tumor tissues were scored as described in Supplementary data. Images shown are representative of three independent experiments.

Figure 8 Schematic model of ER involvement in edelfosine-induced apoptosis in pancreatic cancer cells. This is a schematic diagram designed to portray one currently plausible mechanism of how edelfosine induces apoptosis via ER stress in pancreatic tumor cells. Edelfosine is incorporated into the tumor cell and accumulates in the ER, generating an ER stress response that leads to cell death. See text for details.

Figure 1 - Gajate *et al*.

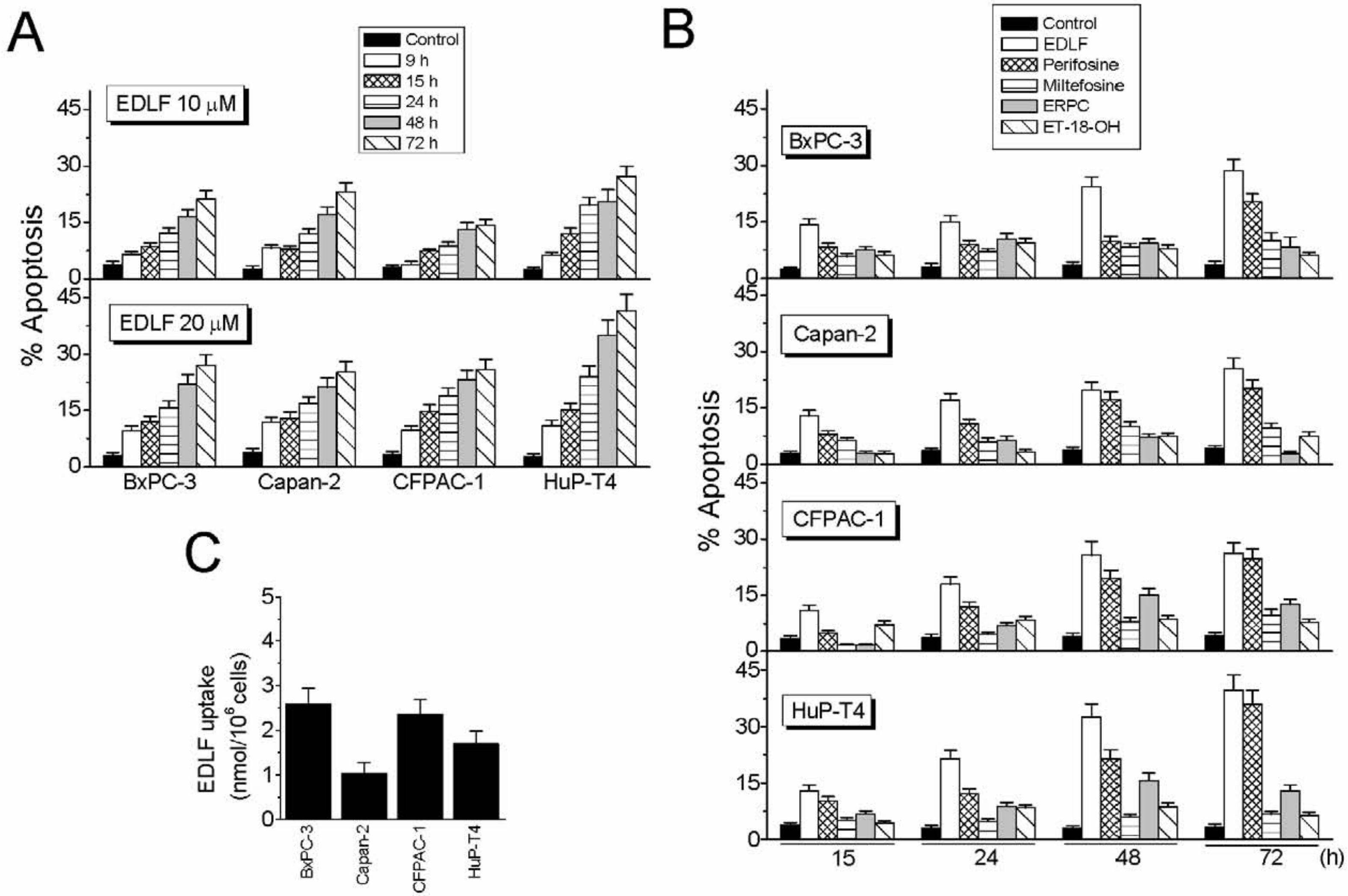

Figure 2 - Gajate *et al*.

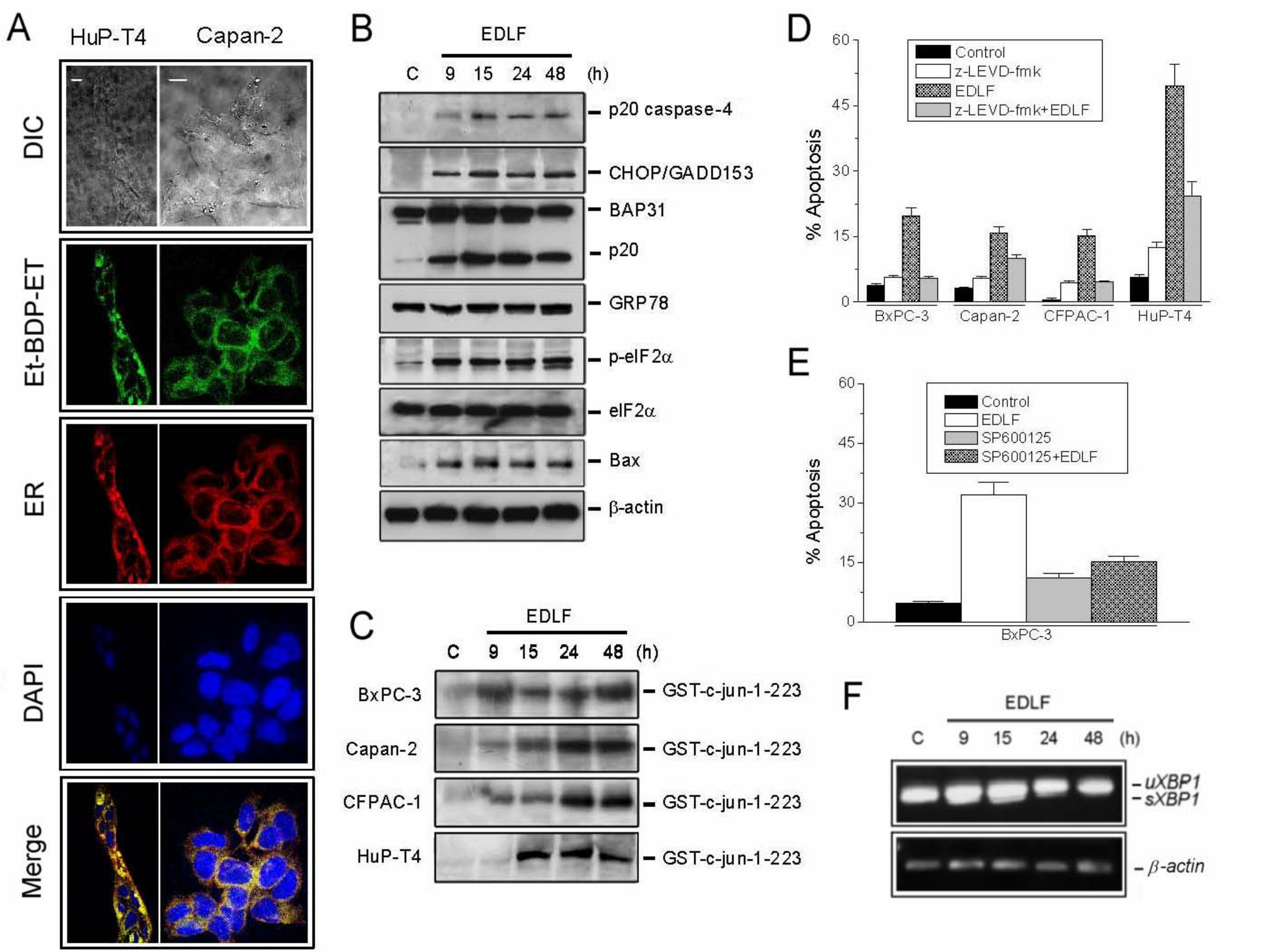

Figure 3 - Gajate *et al*.

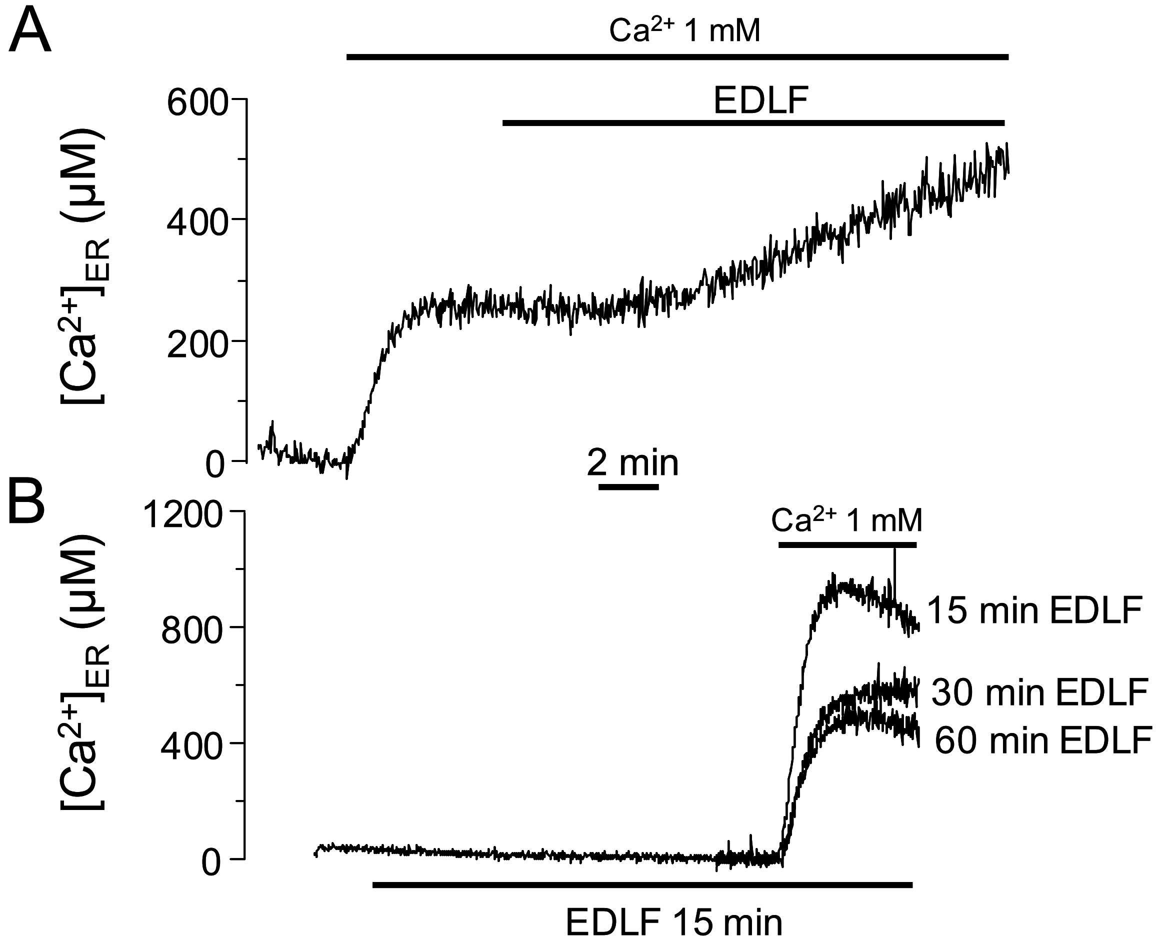

Figure 4 - Gajate *et al*.

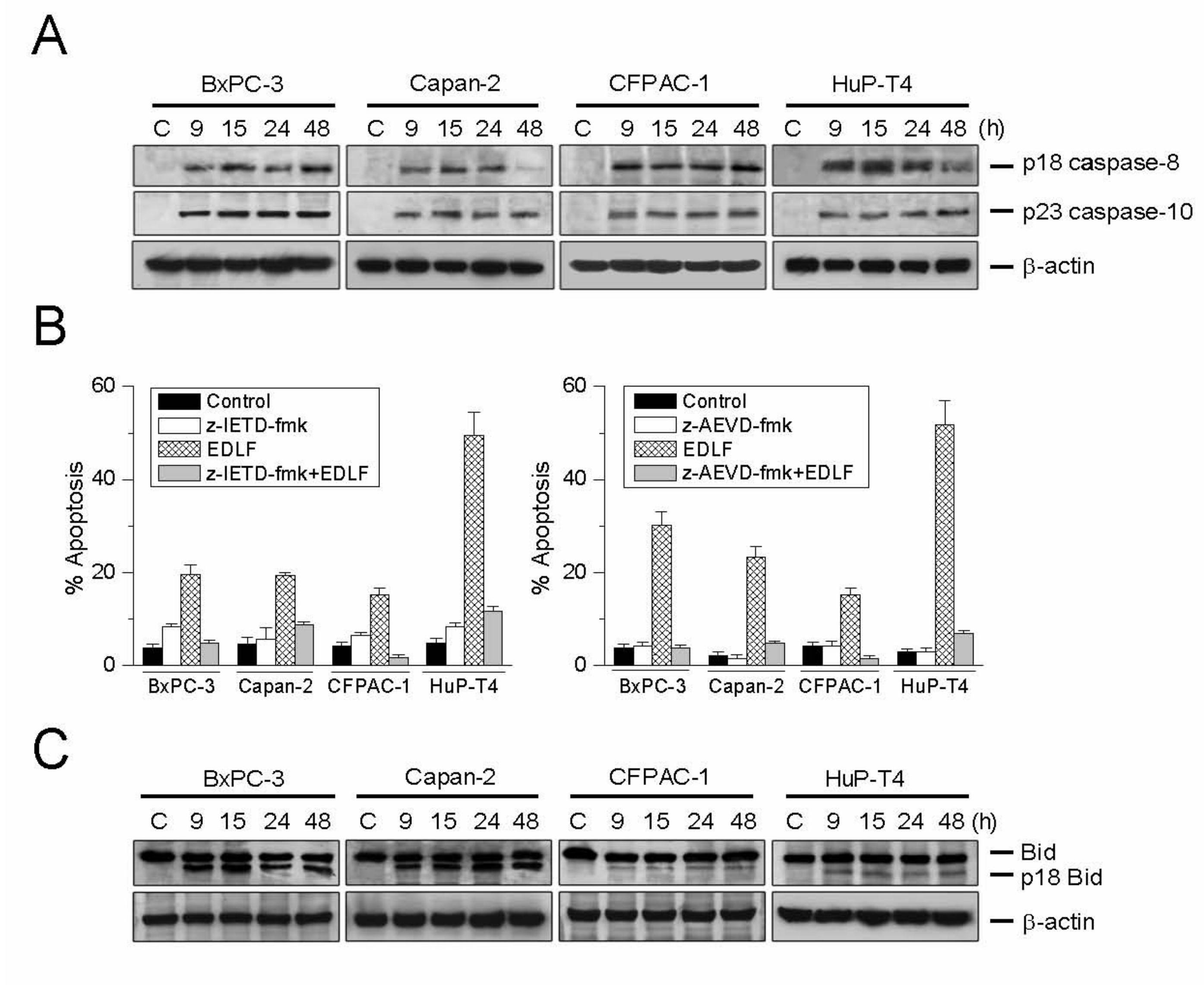

Figure 5 - Gajate *et al*.

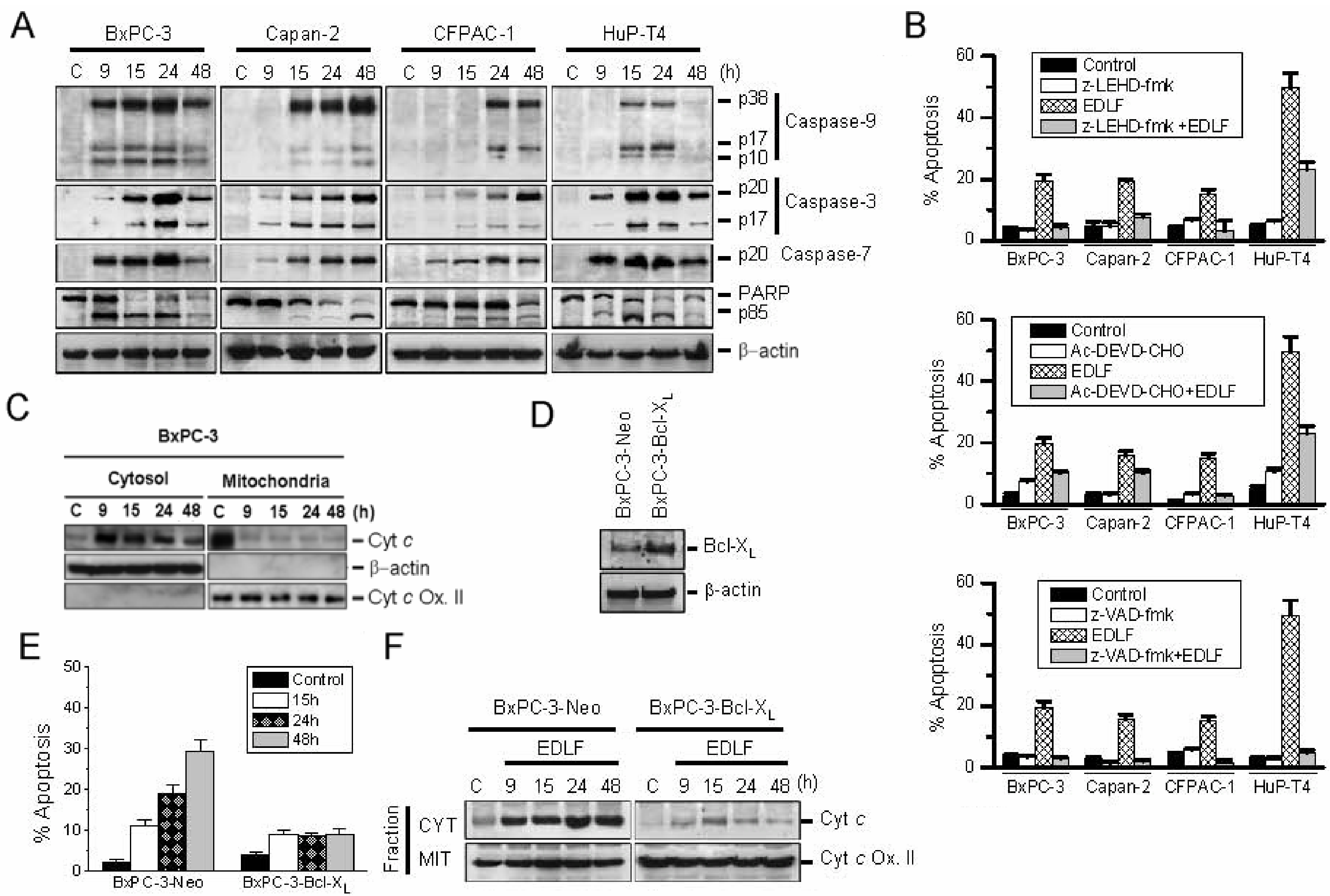

Figure 6 - Gajate *et al*.

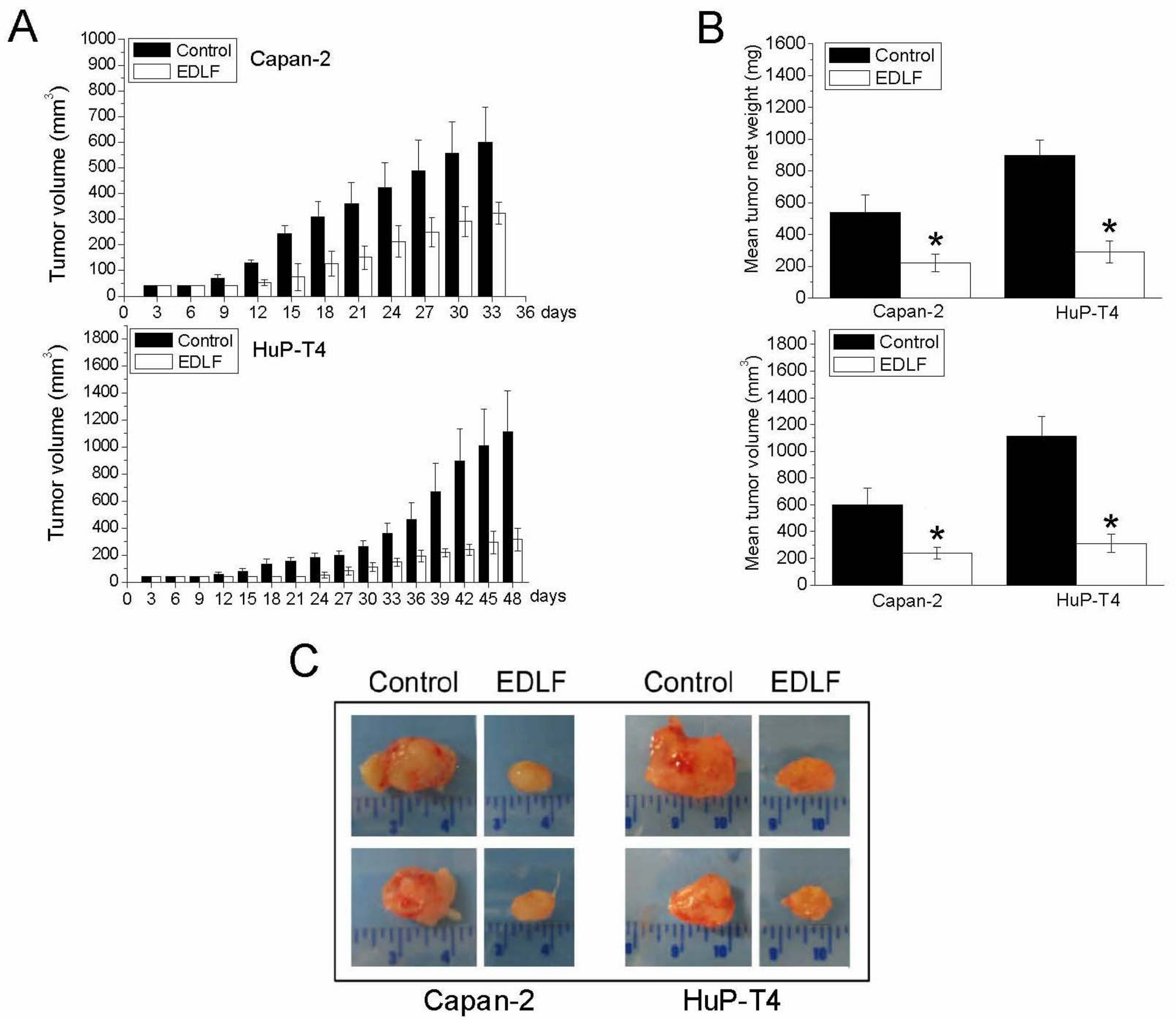

Figure 7 - Gajate *et al*.

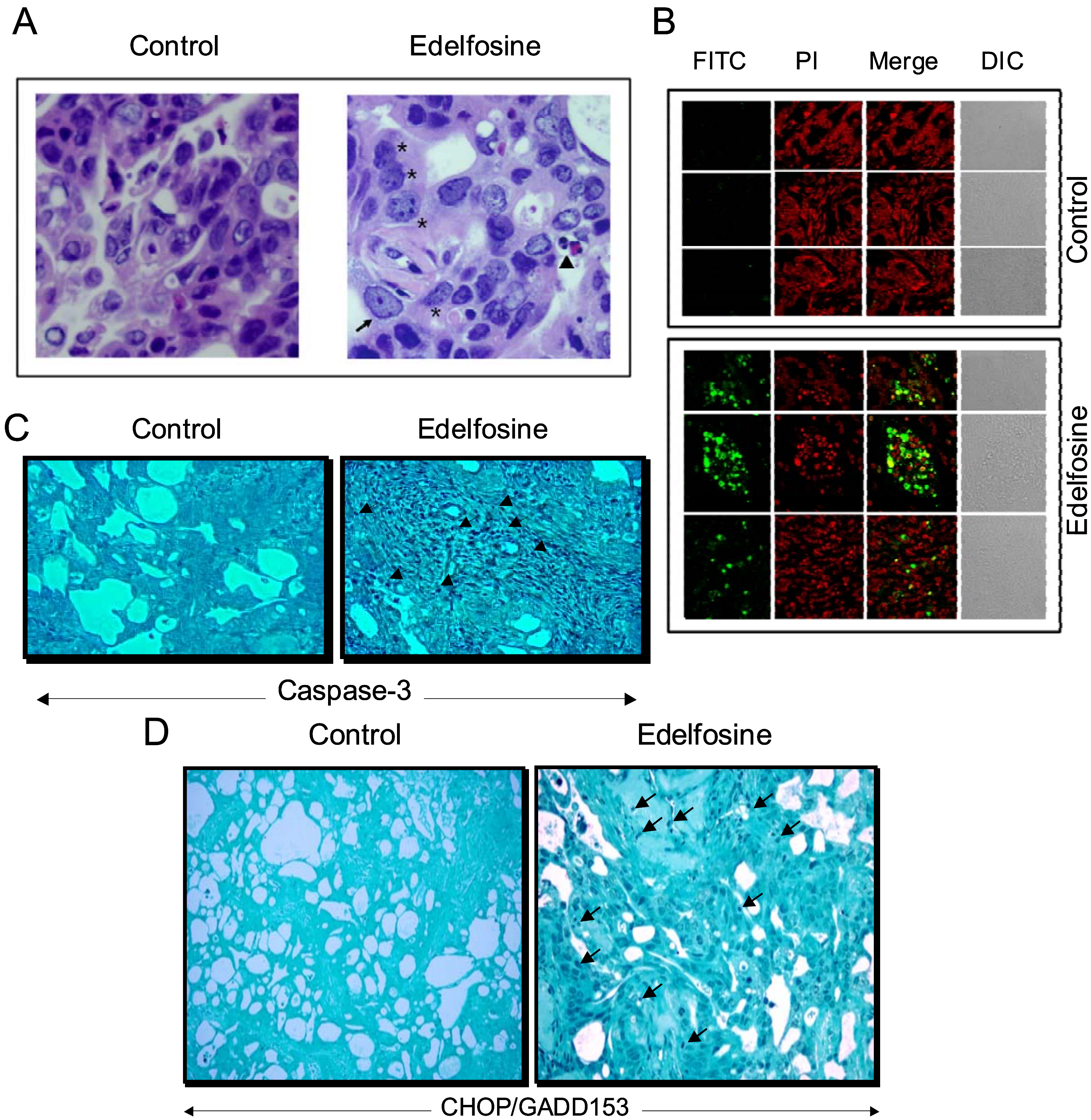

Figure 8 - Gajate *et al*.